Microtubule stabilization in vivo by nucleation-incompetent γ-tubulin complex

Andreas Anders and Kenneth E. Sawin*

Wellcome Trust Centre for Cell Biology, University of Edinburgh, Swann Building, Mayfield Road, Edinburgh EH9 3JR, UK

*Author for correspondence (ken.sawin@ed.ac.uk)

Summary

Although the fission yeast *Schizosaccharomyces pombe* contains many of the γ-tubulin ring complex (γ-TuRC)-specific proteins of the γ-tubulin complex (γ-TuC), several questions about the organizational state and function of the fission yeast γ-TuC in vivo remain unresolved. Using 3×GFP-tagged γ-TuRC-specific proteins, we show here that γ-TuRC-specific proteins are present at all microtubule organizing centers in fission yeast and that association of γ-TuRC-specific proteins with the γ-tubulin small complex (γ-TuSC) does not depend on Mto1, which is a key regulator of the γ-TuC. Through sensitive imaging in *mto1Δ* mutants, in which cytoplasmic microtubule nucleation is abolished, we unexpectedly found that γ-TuC incapable of nucleating microtubules can nevertheless associate with microtubule minus-ends in vivo. The presence of γ-TuC at microtubule ends is independent of γ-TuRC-specific proteins and strongly correlates with the stability of microtubule ends. Strikingly, microtubule bundles lacking γ-TuC at microtubule ends undergo extensive treadmilling in vivo, apparently induced by geometrical constraints on plus-end growth. Our results indicate that microtubule stabilization by the γ-TuC, independently of its nucleation function, is important for maintaining the organization and dynamic behavior of microtubule arrays in vivo.

Key words: Fission yeast, Gamma-tubulin, Microtubules

Introduction

The γ-tubulin complex (γ-TuC) has a crucial role in microtubule (MT) nucleation in eukaryotic cells (Luders and Stearns, 2007; Raynaud-Messina and Merdes, 2007; Wiese and Zheng, 2006). In vertebrates, the γ-TuC consists of multiple copies of the tetrameric γ-tubulin small complex (γ-TuSC), which oligomerize to form a ~2 MDa γ-tubulin ring complex (γ-TuRC), in concert with other proteins (γ-TuRC-specific proteins) (Haren et al., 2006; Hutchins et al., 2010; Luders et al., 2006; Murphy et al., 2001; Oegema et al., 1999; Teixido-Travesa et al., 2010; Zheng et al., 1995). In *Drosophila*, both γ-TuSC and γ-TuRC forms of the γ-TuC can be isolated, although γ-TuRC is much more active than γ-TuSC for MT nucleation in vitro (Oegema et al., 1999). In the fission yeast *Schizosaccharomyces pombe*, both γ-TuSC proteins and γ-TuRC-specific proteins have been identified and characterized (Anders et al., 2006; Fujita et al., 2002; Vardy and Toda, 2000; Venkatram et al., 2004). (The fission yeast homologs of human γ-TuRC-specific proteins GCP4, GCP5 and GCP6 are proteins Gfh1, Mod21 and Alp16, respectively.) This contrasts with the budding yeast *Saccharomyces cerevisiae*, in which only γ-TuSC proteins have been identified (Kollman et al., 2010). However, the in vivo organizational state and function of the fission yeast γ-TuC remains controversial, for several reasons (Anders et al., 2006; Fujita et al., 2002; Venkatram et al., 2004): first, fission yeast γ-TuRC-specific proteins are highly divergent in sequence relative to their higher eukaryotic homologs and to each other, and they appear to lack the 'grip' (gamma-ring protein) motifs shared by many γ-TuC proteins

in higher eukaryotes. Second, although fission yeast γ-TuRC-specific proteins co-immunoprecipitate with γ-TuSC proteins, characterization of the hydrodynamic properties of fission yeast γ-TuC has yielded conflicting results as to whether a large γ-TuRC-like complex exists in fission yeast in vivo; if it does, it might not be very stable upon purification. Third, to date, γ-TuRC-specific proteins have been localized only to a subset of fission yeast microtubule organizing centers (MTOCs): to spindle pole bodies (SPBs) throughout the cell cycle and to equatorial MTOCs during cell division but not, for example, to 'satellite' interphase MTOCs, which are associated with the nuclear envelope and with MTs themselves, and are responsible for most interphase MT nucleation. Finally, deletion of the genes encoding fission yeast γ-TuRC-specific proteins, whether together or in combination, has only relatively mild effects on MT nucleation in vivo. Collectively, these findings have led to a proposal that MT nucleation in fission yeast might depend on a division of labor between γ-TuSC-type complexes and γ-TuRC-type complexes (Anders et al., 2006).

To address these questions, we improved detection of γ-TuRC-specific proteins in fission yeast by tagging them with three copies of GFP. Overall, our data suggest that in vivo, the γ-TuC at fission yeast MTOCs consists of a γ-TuRC-like complex. In addition, however, we identified a previously undescribed localization of the fission yeast γ-TuC to 'free' MT minus-ends in vivo. Further analysis suggests that this localization is important for regulation of the dynamic behavior of MTs, independently of the MT-nucleation function of the γ-TuC.

Results and Discussion

To investigate the state of the fission yeast γ-TuC in vivo, we tagged Gfh1 (GCP4), Mod21 (GCP5) and Alp16 (GCP6) each with three copies of a C-terminal GFP (3×GFP) at their

endogenous chromosomal loci. In strains co-expressing tandem-dimer Tomato-tagged Alp4 (γ-TuSC component, equivalent to human GCP2; Alp4–tdT) (Samejima et al., 2008), 3×GFP-tagged TuRC-specific proteins uniformly colocalized with Alp4–tdT throughout the cell cycle, at spindle pole bodies and equatorial MTOCs as well as at punctate satellites on the nuclear envelope and on MTs (Fig. 1A). This suggests that the fission yeast γ-TuC exists largely as a γ-TuRC-like complex at MTOCs in vivo. Because this complex has not yet been isolated and observed in the electron microscope, at present we refrain from referring to it as fission yeast 'γ-TuRC'.

Previous co-immunoprecipitation experiments suggested specific dependency relationships among fission yeast γ-TuRC-specific proteins for their association with γ-TuSC (Anders et al., 2006). Alp16 is most 'central', because it requires neither Gfh1 nor Mod21 for association with γ-TuSC, but is required for association of both Gfh1 and Mod21 with γ-TuSC. By contrast, Mod21 is most 'peripheral', because it requires both Gfh1 and Alp16 for association with γ-TuSC and is not required for association of either Gfh1 or Alp16 with γ-TuSC. Imaging 3×GFP-tagged γ-TuRC-specific proteins in single- and double-deletion mutants of γ-TuRC-specific proteins revealed similar dependencies, confirming co-immunoprecipitation results (Anders et al., 2006) and further demonstrating that dependencies apply equally to all types of MTOCs (see supplementary material Fig. S1).

In fission yeast, localization of γ-TuC to prospective cytoplasmic MTOCs requires interaction with the Mto1/2 complex, which contains the proteins Mto1 and Mto2, localizes to prospective MTOCs independently of its interaction with γ-TuC (Janson et al., 2005; Samejima et al., 2005; Samejima et al., 2008; Samejima et al., 2010; Sawin et al., 2004; Venkatram et al., 2004). In *mto1Δ* cells, de novo cytoplasmic MT nucleation is completely abolished, whereas in *mto2Δ* cells, Mto1-dependent cytoplasmic nucleation can occur, but only from the SPB. Because Mto1/2 appears to be crucial not only for the localization of the γ-TuC but also for its activity, we tested whether Mto1/2 contributes to the integrity of the γ-TuC. We found that 3×GFP–tagged γ-TuRC-specific proteins co-immunoprecipitated HA-tagged Alp4 equally well in wild-type and in *mto1Δ* strains (Fig. 1C). We confirmed this by imaging γ-TuRC-specific proteins with Alp4 in *mto1Δ* mutants. As in wild-type cells, γ-TuRC-specific proteins in *mto1Δ* cells colocalized with Alp4 (Fig. 1B), although because of *mto1Δ* MT defects, localization in the mutant was limited primarily to the intranuclear face of the SPB and a few faint cytoplasmic puncta (see below). Collectively, these results indicate that in fission yeast, a γ-TuRC-like complex exists as a stable structure in vivo independent of the Mto1/2 complex.

The faint γ-TuC puncta seen in *mto1Δ* mutants were, however, unexpected. They have not been seen before (Zimmerman and Chang, 2005), probably because of their very faint signal. Because they contained both Alp4 and γ-TuRC-specific proteins, they were unlikely to be artifactual or background fluorescence. We therefore investigated these puncta more closely, to determine whether they were associated with any particular structure.
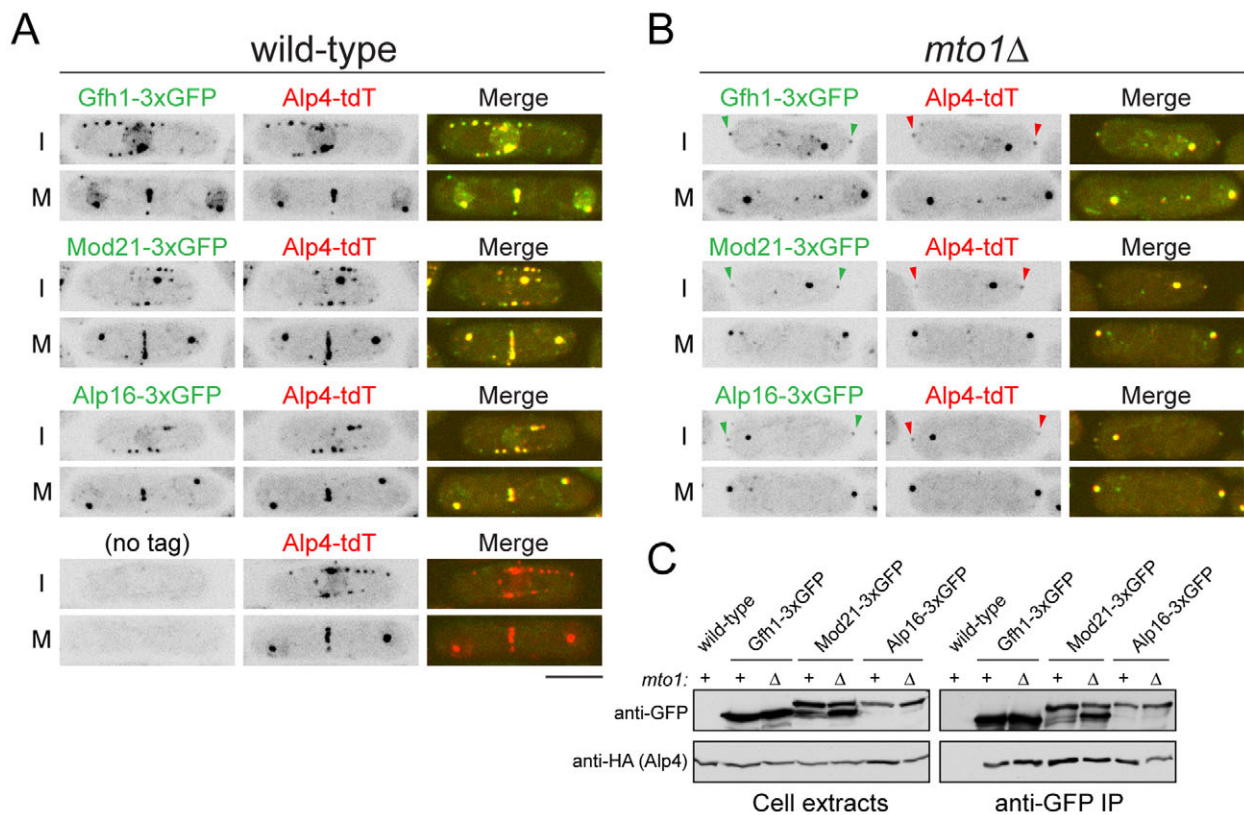
Fig. 1. Colocalization of γ-TuRC-specific and γ-TuSC proteins at fission yeast MTOCs. (A,B) Colocalization of the indicated 3×GFP–tagged γ-TuRC-specific proteins with tandem-dimer Tomato-tagged TuSC protein Alp4 (Alp4–tdT) in (A) wild-type and (B) *mto1Δ* cells. I, interphase cells; M, mitotic cells. Arrowheads in B show examples of faint puncta containing both γ-TuRC-specific and γ-TuSC proteins in *mto1Δ* cells. Scale bar: 5 μm. **(C)** Anti-GFP and anti-HA western blots showing co-immunoprecipitation of HA-tagged Alp4 with 3×GFP-tagged γ-TuRC-specific proteins in both wild-type and *mto1Δ* cells.
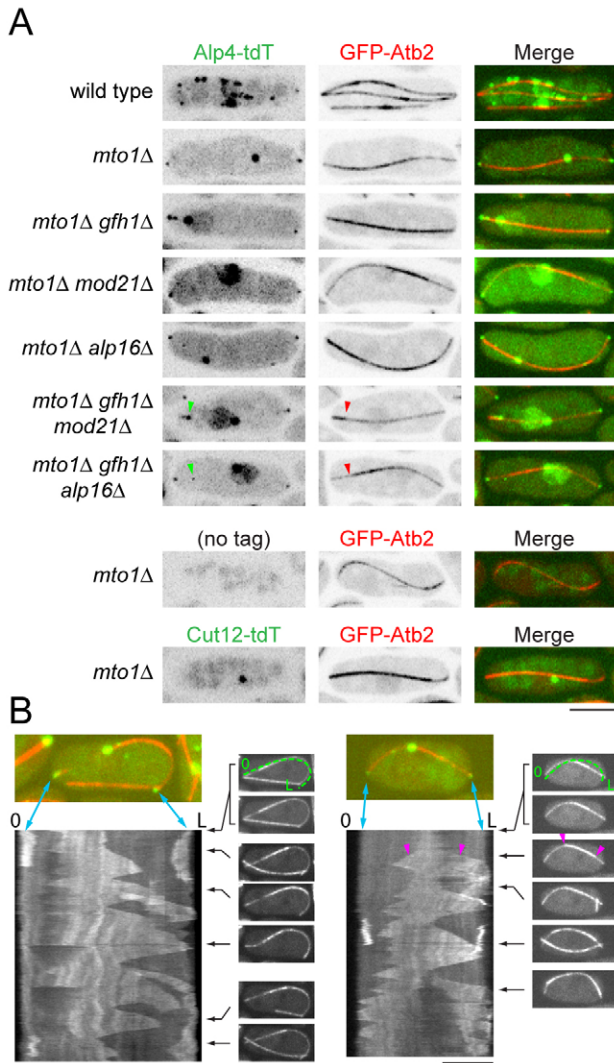
Fig. 2. γ-tubulin complex puncta in *mto1Δ* cells are associated with microtubule minus-ends, independently of γ-TuRC-specific proteins. (**A**) Tandem-dimer Tomato-tagged γ-TuSC protein Alp4 (Alp4–tdT) and GFP–tubulin (GFP–Atb2) in interphase cells of the indicated genotypes. Arrowheads show examples of puncta on MT ends within bundles; slight misregistrations are due to movement during imaging. No comparable puncta are seen in negative-control cells lacking tdT-tagged protein ('no tag') or containing tdT-tagged SPB marker Cut12. (**B**) Kymographs of GFP–Atb2 dynamics in *mto1Δ* cells, of MT bundles with γ-TuC puncta at both ends. Two-color images show γ-TuC (Alp4–tdT; green) localization at ends of bundles (GFP–Atb2; red), before time-lapse imaging of GFP–Atb2 (kymograph and selected still-images). Dashed green lines ('0' to 'L') in still-images at first time point indicate kymograph *x*-axis. Double-headed blue arrows show how positions of bundle ends in images are related to points along kymograph *x*-axis (horizontal axis). Magenta arrowheads in right-hand panels show example of microtubule overlap zone in kymograph and still images. Total time in kymograph is 12 minutes (vertical axis). Scale bars: 5 μm (bar in B applies to two-color images and kymographs only).

Interestingly, we found that γ-TuC puncta in *mto1Δ* cells were specifically associated with the ends of MT bundles (Fig. 2A). Although *mto1Δ* mutants are completely defective in de novo cytoplasmic MT nucleation, mutant cells often contain one or two bundles of cytoplasmic MTs, which are due to the 'escape' of

intranuclear MTs from the nucleus at the end of mitosis (Sawin et al., 2004; Zimmerman and Chang, 2005). In many (but not all) cells, puncta were seen at both ends of bundles, and when puncta were observed along the length of bundles, these correlated with the ends of individual MTs within the bundle (Fig. 2A; see also Fig. 3A,C). Further control experiments indicated that the puncta are not 'remnants' of the SPBs and are independent of the specific tags used (see supplementary material Fig. S2).

Based on the known role of the γ-TuC in MT nucleation, the most likely interpretation of this localization was that these γ-TuC puncta are at MT minus-ends. We confirmed this by analyzing MT dynamics in bundles with puncta at each end, which would be expected to have an antiparallel organization. Although many of these bundles were very stable, kymograph analysis revealed dynamic behavior characteristic of MT plus-ends at the 'free' MT ends in the overlap region of some bundles, whereas the inferred minus-ends associated with puncta in the same bundles did not show similar behavior (Fig. 2B; supplementary material Movies 1 and 2). Deletion of γ-TuRC-specific proteins (in the *mto1Δ* strain background) did not affect association of puncta with MT ends (Fig. 2A). Taken together, these results indicate that even when completely incapable of nucleating MTs, γ-TuCs can nevertheless associate with MT minus-ends in vivo, and this ability is common to both γ-TuRC-like complexes and γ-TuSCs.

The apparent stability of γ-TuC-associated minus-ends in antiparallel MT bundles in *mto1Δ* cells led us to examine more generally whether association of γ-TuCs with minus-ends conferred stability, under conditions where we could continually visualize both MTs and γ-TuCs. In spite of their faint signal, γ-TuC puncta could be imaged together with GFP–tubulin for up to ~12 minutes (30 time points) before photobleaching prevented further imaging. We found that nearly all MT ends associated with γ-TuCs were stable over this period, whereas ends lacking γ-TuCs showed dynamic behavior (Fig. 3A–C, Fig. 3E; supplementary material Movies 3–5). This suggests that association with γ-TuC can stabilize minus-ends, even when the γ-TuC is incapable of MT nucleation. Similar results were obtained in *mto1Δ alp16Δ* double mutants, in which γ-TuRC-specific proteins do not associate with γ-TuSC (Anders et al., 2006), indicating that a γ-TuRC-like complex per se is not required for minus-end stability; γ-TuSC is sufficient (Fig. 3D,E; supplementary material Movie 6).

Our results have two important implications. First, they help to explain the complex MT dynamics observed in *mto1Δ* mutants (Sawin et al., 2004; Zimmerman and Chang, 2005). In addition to their unusual intranuclear origin, cytoplasmic MT bundles in *mto1Δ* cells are typically more kinetically stable than in wild-type cells, with individual bundles often persisting for tens of minutes. In spite of this stability, MTs in *mto1Δ* cells can still show a variety of dynamic behavior, including growth, shrinkage and pausing, as well as bend-breakage events, during which MTs at cell tips curl around the inside of the cell tip and, instead of undergoing catastrophe as in wild-type cells, break in half as a result of bending stress (Sawin et al., 2004; Venkatram et al., 2004; Zimmerman and Chang, 2005). Our results suggest that the presence or absence of γ-TuCs at MT minus-ends is an important factor that influences overall MT behavior in vivo. Good examples of this are the stable antiparallel MT bundles with γ-TuCs at each end. By contrast, MTs generated by bend-breakage events lack γ-TuC at their ends and are often short-lived, as a result of rapid depolymerization (Sawin et al., 2004; Zimmerman and Chang, 2005) (supplementary material Movies 2, 3 and 8). Some MTs in
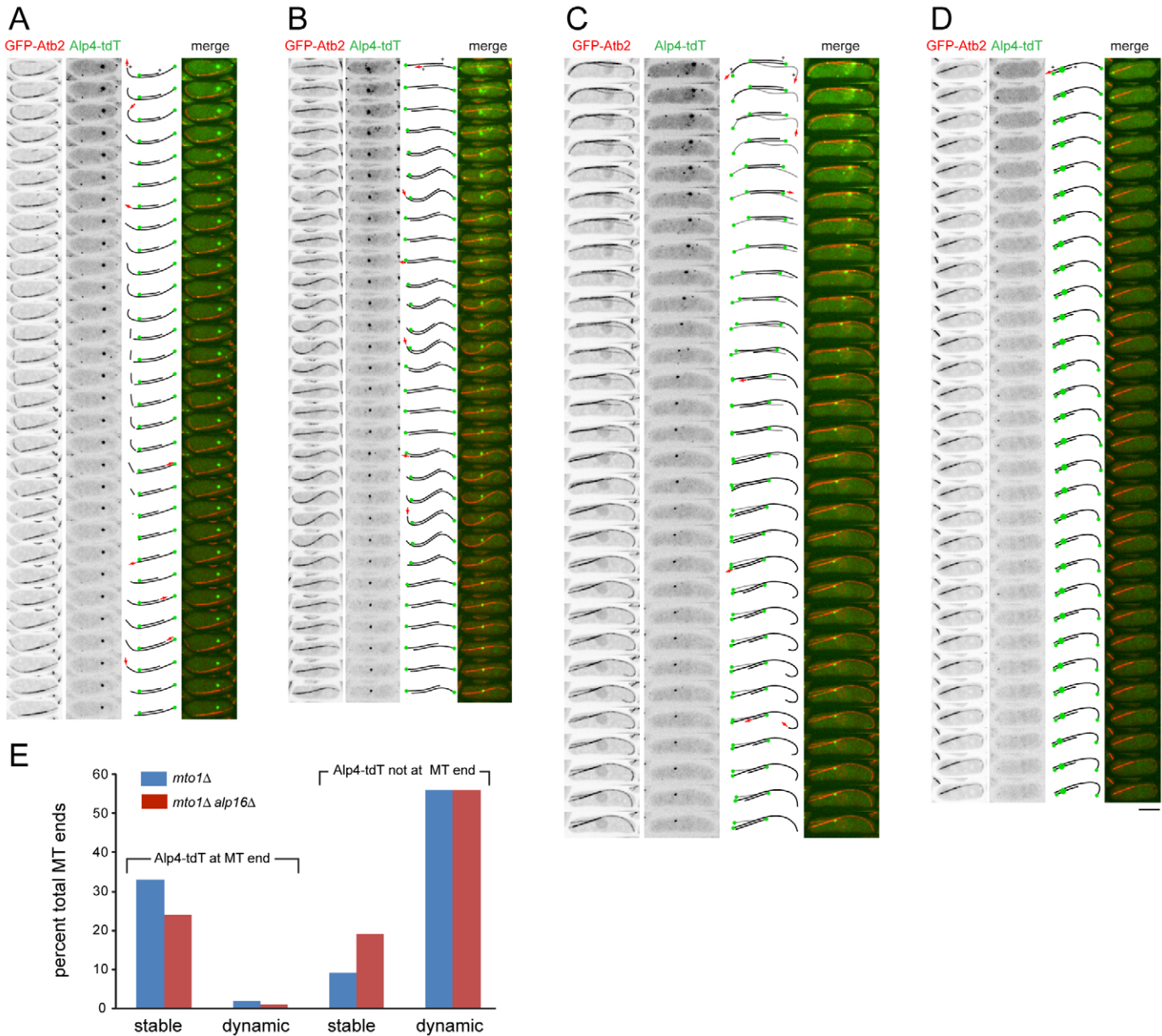
Fig. 3. γ-tubulin complex puncta in *mto1Δ* cells are associated with stable microtubule ends. (A–D) GFP–tubulin and Alp4–tdT dynamics in interphase (A–C) *mto1Δ* and (D) *mto1Δ alp16Δ* cells. Images are shown at 25 second intervals; total elapsed time 12 minutes. In each panel, individual channels, merged images and cartoons are shown. The most intense spot in each Alp4–tdT time-series is the spindle pole body. Green dots in cartoons indicate γ-TuC at minus-ends. Red arrows indicate growth and shrinkage of the indicated MTs. Large green dot in D represents the SPB. In A, plus-end of MT nucleated from right-hand side repeatedly attempts to grow against the left-hand cell tip, resulting in shrinking and/or bend-breakage as MT curves around tip. In B, plus-end of MT nucleated from right-hand side grow against the left-hand cell tip, generating force that buckles the MT bundle; subsequent shrinking at the same plus-end relaxes the buckling. This happens three times in succession. In C, plus-end of MT nucleated from left-of-center of cell grows against right-hand cell tip, pushing the MT bundle leftwards. Once the bundle is pushed all the way against the left-hand cell tip, this same plus-end grows to curve around cell tip. In D, the plus-end of the MT nucleated from right-hand side grows against left-hand cell tip, bending the MT bundle. **(E)** Quantification of stability of MT ends containing or lacking γ-TuC (Alp4–tdT), in *mto1Δ* and *mto1Δ alp16Δ* cells, determined from time-lapse imaging of the type shown in A–D. The relatively high number of stable ends without Alp4–tdT in *mto1Δ alp16Δ* mutants might be due to our inability to detect very low amounts of γ-TuSC that are nevertheless sufficient for stabilization (see Materials and Methods).

mto1Δ cells have also been observed to undergo treadmilling (Rodionov and Borisy, 1997; Zimmerman and Chang, 2005). We re-investigated this and found a strong positive correlation between treadmilling behavior and the absence of γ-TuCs from the ends of MT bundles (Fig. 4A–C; supplementary material Movies 7 and 8; this is not in conflict with data in Fig. 3 because most treadmilling bundles eventually convert to growing or shrinking bundles; data

not shown). Interestingly, we also found that nearly all treadmilling was observed in the context of MT bundles in which apparently stationary ends were constrained by cell geometry (e.g. MTs extending from one cell tip to another, or across the cell diameter) (Fig. 4B). Bundles that escaped this geometric constraint immediately stopped treadmilling, even though polymerization at plus-ends continued (Fig. 4D; supplementary material Movie 9).
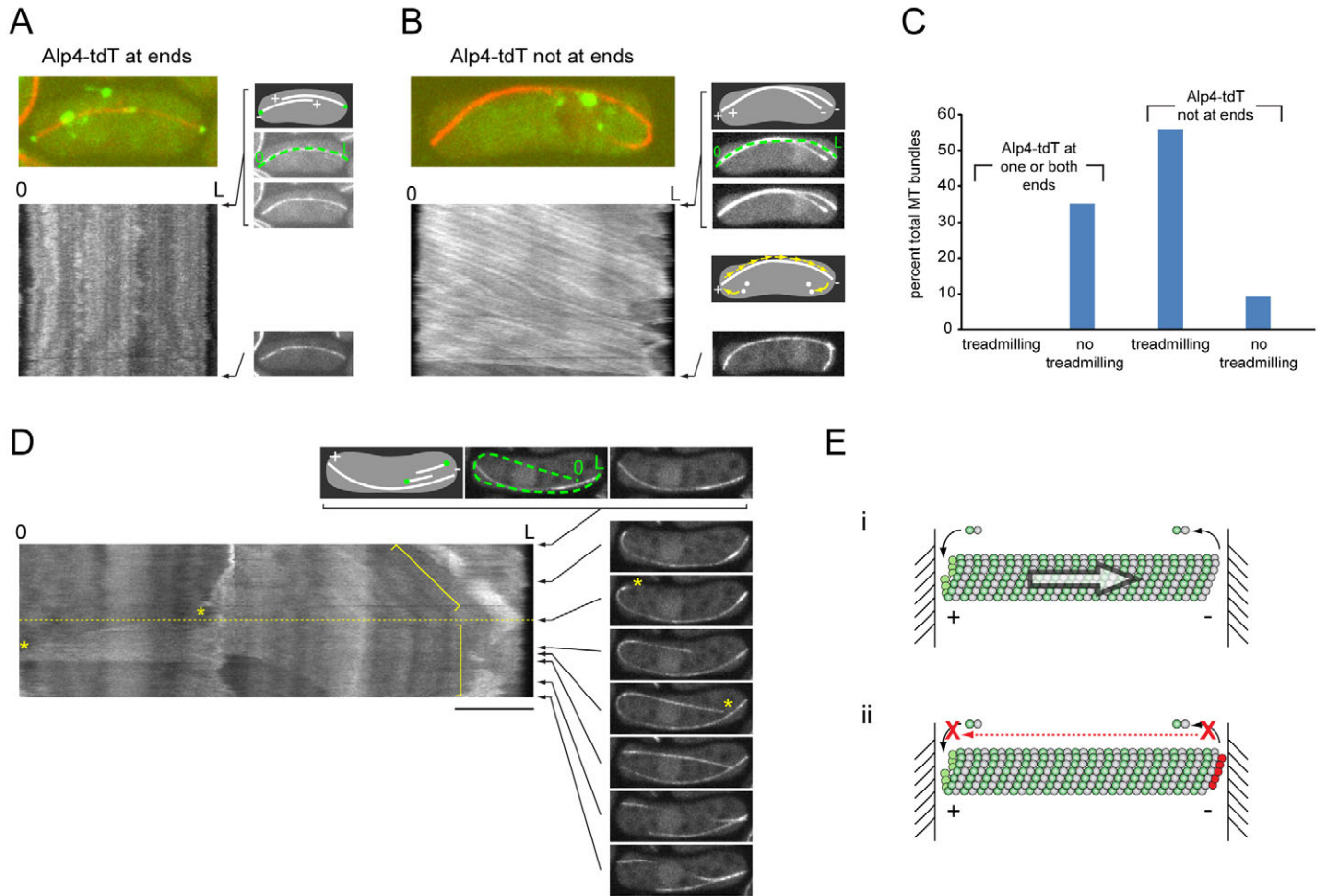
Fig. 4. Microtubule treadmilling in *mto1Δ* cells when γ-tubulin complex puncta are absent from microtubule ends. (**A**,**B**) Still images and kymographs of MT dynamics in cells with (A) Alp4–tdT puncta at both ends of an antiparallel MT bundle and (B) no Alp4–tdT at either end of a parallel bundle. Labeling is as in Fig. 2; cartoons accompanying still images show inferred MT polarity. In B, movement of lattice-incorporated GFP–tubulin from plus-end '0' towards minus-end 'L' indicates treadmilling via tubulin incorporation at plus-ends accompanied by disassembly at minus-ends (cartoon). Total time in each kymograph in A and B is 6 minutes 40 seconds (vertical axis). (**C**) Quantification of treadmilling in MT bundles containing or lacking γ-TuC (Alp4–tdT) at ends. (**D**) Treadmilling occurs when cellular geometry constrains MT growth. Portion of kymograph from a cell with a parallel bundle. Initially net growth is blocked by cell tips acting as barriers, and treadmilling occurs towards minus-end 'L' (diagonal bracket). Once the MT plus-end becomes free from this constraint (dashed line), it begins to grow (see corresponding asterisks in stills and kymographs), and at the same time, treadmilling stops (vertical bracket). Total time in kymograph is 6 minutes. (**E**) Speculative model for barrier-induced treadmilling in vivo. (i) When γ-TuCs are absent from MT minus-ends, incorporation of new tubulin subunits at plus-ends results in a compressive force, which pushes minus-ends towards disassembly. (ii) When γ-TuCs (red spheres) are present at minus-ends, disassembly is blocked. As a result, effects of compressive forces on assembly and/or disassembly are 'felt' at plus-ends, indirectly leading to reduced subunit incorporation at plus-ends.

This observation of 'barrier-induced treadmilling', generated by cell structure, might be of particular interest from the perspective of mechanical control of MT dynamics (Laan and Dogterom, 2010; Tischer et al., 2009), because it suggests that forces produced by polymerization at plus-ends are sufficient to cause depolymerization at minus-ends under conditions where such depolymerization might not otherwise occur (Fig. 4E). Thermodynamically, the energy driving depolymerization would ultimately be derived from GTP hydrolysis; related to this, treadmilling within barriers has been shown to be capable of producing useful mechanical work (Hill and Kirschner, 1982). Conversely, when γ-TuC is bound to minus-ends, inhibition of minus-end depolymerization might indirectly impede plus-end polymerization against a barrier (Fig. 4E). In such cases, limited plus-end polymerization might occur, which leads to MT buckling and increased compressive forces on plus-ends and, ultimately,

transition to MT shrinkage (supplementary material Movies 3–5) (Janson et al., 2003).

Second, our results also have a broader general significance for understanding the regulation of MT dynamics in vivo. Previous in vitro experiments showed that *Xenopus* γ-TuRC can bind and stabilize MT minus-ends without having nucleated them (Wiese and Zheng, 2000). However, the in vivo relevance of these experiments has, until now, remained unclear. In addition, although γ-TuRC in these earlier experiments was added to pre-assembled MTs and thus stabilized MTs 'independently' of nucleation, the γ-TuRC used was nevertheless competent for assembly. Our finding that the γ-TuC, and specifically γ-TuSC, can stabilize 'free' MT ends in vivo, independently of any nucleating activity or of active MTOCs, suggests that MT stabilization by the γ-TuC is mechanistically distinct from nucleation by the γ-TuC. We propose that minus-end capping by γ-TuC is important for MT stability

away from nucleation sites, which might occur, for example, after release from these sites (Bellett et al., 2009; Moss et al., 2007; Rodionov and Borisy, 1997).

Recent experiments in *Drosophila* have suggested that MT lattice-associated γ-TuRC contributes to MT stabilization, possibly by promoting either a transient or long-lasting paused state (Bouissou et al., 2009). These results are not incompatible with our own, but they are fundamentally different: in particular, in our system γ-TuC is not lattice-associated but rather is found only at minus-ends, and the mechanism of MT stabilization is thus likely to be different. Such differences emphasize the view that γ-TuC might act in various ways, in different cell types, to effect stereotyped patterns of MT organization in vivo.

Materials and Methods

Yeast strains
Standard yeast methods were used throughout (Moreno et al., 1991). Strains are listed in supplementary material Table S1.

Genetic and biochemical methods
All gene tagging was at chromosomal loci (Bahler et al., 1998). Apart from *nmt81*:GFP-Atb2, proteins were tagged at the C-terminus and expressed from endogenous promoters. 3×GFP tagging of γ-TuRC-specific proteins Gfh1, Mod21 and Alp16 was carried out by subcloning the relevant 500 bp homology-sequences of γ-TuRC-specific genes into 3×GFP tagging plasmid pSM458 (Martin and Chang, 2006), followed by transformation and homologous recombination. Integration was verified by colony PCR and western blotting. Immunoprecipitation experiments were performed as described previously, using cells frozen in liquid nitrogen and ground to a powder while frozen (Anders et al., 2006). Homemade sheep anti-GFP and 12CA5 mouse anti-HA were used.

Microscopy
Cells were grown at 25°C in EMM2 minimal medium and imaged live as described (Snaith et al., 2010). With one exception (see below), all imaging used a confocal spinning disk microscope with 488 nm and 561 nm lasers, at room temperature, as described (Bicho et al., 2010). For two-channel single time-point imaging of 3×GFP–tagged γ-TuRC-specific proteins with Alp4–tdTomato (Fig. 1), seven *Z*-sections at 0.6 µm spacing were collected simultaneously in GFP and RFP channels (19 mW at 488 nm, 4.5 mW at 561 nm, 1500 ms exposure) using an Optosplit III image splitter (Cairn). For two-channel still and time-lapse imaging of GFP–Atb2 and Alp4–tdT (Figs 2 and 3), seven *Z*-sections at 0.6 µm spacing were collected every 25 seconds (5 mW at 488 nm, 250 ms exposure per section for GFP; 3.75 mW at 561 nm, 3000 ms for tdTomato), for 30 time points (12 minutes). For single-channel time-lapse imaging of GFP–Atb2 in *mto1Δ* (Figs 2, 4), seven *Z*-sections at 0.6 µm spacing were collected every 3 seconds (7 mW at 488 nm, 300 ms exposure per section), for 240 time points (12 minutes).

Imaging of 3×GFP–tagged γ-TuRC-specific proteins with Alp4–tdT in deletion-mutants of γ-TuRC (supplementary material Fig. S1) used wide-field microscopy as described previously (Sawin et al., 2004; Snaith and Sawin, 2003). Six *Z*-sections at 0.6 µm spacing were collected at a single time point (1000 ms exposure per section for 3×GFP, 800 ms for tdTomato), with appropriate neutral density filters to minimize photobleaching.

Kymographs and movies were created using Metamorph software. Merged images were generated using Photoshop (Adobe). All image processing used strictly linear contrast. In all cases maximum projections of Z-series are shown.

Quantification of MTs
For quantification of stable and dynamic MT ends containing or lacking γ-TuCs (Fig. 3), 231 and 205 MT ends were analysed from movies of GFP–Atb2 and Alp4–tdT tagged *mto1Δ* and *mto1Δ alp16Δ* cells, respectively. MT ends showing any significant growth or shrinkage during the imaging period (12 minutes) were scored as dynamic. In clear instances of sliding of stable MTs, ends were scored as stable. In cases where a stable end was clearly moving as a result of pushing from polymerization at the other end at the cell tip (which can be inferred from buckling of the bundle), the stable end was scored as stable, and the polymerizing was scored as dynamic. If there were any doubts, the moving end was scored as dynamic. Some of the apparently stable ends lacking Alp4–tdTomato might represent occasional mis-scored MT ends that contain Alp4–dtTomato but failed to produce a signal that was sufficiently strong for detection (especially in *mto1Δ alp16Δ* double mutants).

For measurement of treadmilling MTs in *mto1Δ* cells (Fig. 4), 55 MT bundles were analysed from GFP–Atb2 movies. Before single-channel GFP–Atb2 time-lapse imaging, a two-channel Alp4–tdT and GFP–Atb2 image was acquired to determine presence or absence of γ-TuCs at MT ends. Treadmilling was evaluated by visual inspection and by kymographs, specifically in the first 1–2 minutes of imaging, and

only in bundles for which γ-TuC presence or absence could be observed before time-lapse imaging (e.g. new bundles that appeared in the time-lapse sequence as a result of MT bend-breakage were not included in the analysis).

Supplementary material available online at
http://jcs.biologists.org/cgi/content/full/124/8/1207/DC1

References

Anders, A., Lourenco, P. C. and Sawin, K. E. (2006). Noncore components of the fission yeast gamma-tubulin complex. *Mol. Biol. Cell* **17**, 5075-5093.

Bahler, J., Wu, J. Q., Longtine, M. S., Shah, N. G., McKenzie, A., 3rd, Steever, A. B., Wach, A., Philippsen, P. and Pringle, J. R. (1998). Heterologous modules for efficient and versatile PCR-based gene targeting in Schizosaccharomyces pombe. *Yeast* **14**, 943-951.

Bellett, G., Carter, J. M., Keynton, J., Goldspink, D., James, C., Moss, D. K. and Mogensen, M. M. (2009). Microtubule plus-end and minus-end capture at adherens junctions is involved in the assembly of apico-basal arrays in polarised epithelial cells. *Cell Motil. Cytoskeleton* **66**, 893-908.

Bicho, C. C., Kelly, D. A., Snaith, H. A., Goryachev, A. B. and Sawin, K. E. (2010). A catalytic role for Mod5 in the formation of the Tea1 cell polarity landmark. *Curr. Biol.* **20**, 1752-1757.

Bouissou, A., Verollet, C., Sousa, A., Sampaio, P., Wright, M., Sunkel, C. E., Merdes, A. and Raynaud-Messina, B. (2009). {gamma}-Tubulin ring complexes regulate microtubule plus end dynamics. *J. Cell Biol.* **187**, 327-334.

Fujita, A., Vardy, L., Garcia, M. A. and Toda, T. (2002). A fourth component of the fission yeast gamma-tubulin complex, Alp16, is required for cytoplasmic microtubule integrity and becomes indispensable when gamma-tubulin function is compromised. *Mol. Biol. Cell* **13**, 2360-2373.

Haren, L., Remy, M. H., Bazin, I., Callebaut, I., Wright, M. and Merdes, A. (2006). NEDD1-dependent recruitment of the gamma-tubulin ring complex to the centrosome is necessary for centriole duplication and spindle assembly. *J. Cell Biol.* **172**, 505-515.

Hill, T. L. and Kirschner, M. W. (1982). Subunit treadmilling of microtubules or actin in the presence of cellular barriers: possible conversion of chemical free energy into mechanical work. *Proc. Natl. Acad. Sci. USA* **79**, 490-494.

Hutchins, J. R., Toyoda, Y., Hegemann, B., Poser, I., Heriche, J. K., Sykora, M. M., Augsburg, M., Hudecz, O., Buschhorn, B. A., Bulkescher, J. et al. (2010). Systematic analysis of human protein complexes identifies chromosome segregation proteins. *Science* **328**, 593-599.

Janson, M. E., de Dood, M. E. and Dogterom, M. (2003). Dynamic instability of microtubules is regulated by force. *J. Cell Biol.* **161**, 1029-1034.

Janson, M. E., Setty, T. G., Paoletti, A. and Tran, P. T. (2005). Efficient formation of bipolar microtubule bundles requires microtubule-bound gamma-tubulin complexes. *J. Cell Biol.* **169**, 297-308.

Kollman, J. M., Polka, J. K., Zelter, A., Davis, T. N. and Agard, D. A. (2010). Microtubule nucleating gamma-TuSC assembles structures with 13-fold microtubule-like symmetry. *Nature* **466**, 879-882.

Laan, L. and Dogterom, M. (2010). In vitro assays to study force generation at dynamic microtubule ends. *Methods Cell Biol.* **95**, 617-639.

Luders, J. and Stearns, T. (2007). Microtubule-organizing centres: a re-evaluation. *Nat. Rev. Mol. Cell Biol.* **8**, 161-167.

Luders, J., Patel, U. K. and Stearns, T. (2006). GCP-WD is a gamma-tubulin targeting factor required for centrosomal and chromatin-mediated microtubule nucleation. *Nat. Cell Biol.* **8**, 137-147.

Martin, S. G. and Chang, F. (2006). Dynamics of the formin for3p in actin cable assembly. *Curr. Biol.* **16**, 1161-1170.

Moreno, S., Klar, A. and Nurse, P. (1991). Molecular analysis of the fission yeast *Schizosaccharomyces pombe. Methods Enzymol.* **194**, 795-823.

Moss, D. K., Bellett, G., Carter, J. M., Liovic, M., Keynton, J., Prescott, A. R., Lane, E. B. and Mogensen, M. M. (2007). Ninein is released from the centrosome and moves bi-directionally along microtubules. *J. Cell Sci.* **120**, 3064-3074.

Murphy, S. M., Preble, A. M., Patel, U. K., O'Connell, K. L., Dias, D. P., Moritz, M., Agard, D., Stults, J. T. and Stearns, T. (2001). GCP5 and GCP6: two new members of the human gamma-tubulin complex. *Mol. Biol. Cell* **12**, 3340-3352.

Oegema, K., Wiese, C., Martin, O. C., Milligan, R. A., Iwamatsu, A., Mitchison, T. J. and Zheng, Y. (1999). Characterization of two related Drosophila gamma-tubulin complexes that differ in their ability to nucleate microtubules. *J. Cell Biol.* **144**, 721-733.

Raynaud-Messina, B. and Merdes, A. (2007). Gamma-tubulin complexes and microtubule organization. *Curr. Opin. Cell Biol.* **19**, 24-30.

Rodionov, V. I. and Borisy, G. G. (1997). Microtubule treadmilling in vivo. *Science* **275**, 215-218.

Samejima, I., Lourenco, P. C., Snaith, H. A. and Sawin, K. E. (2005). Fission yeast mto2p regulates microtubule nucleation by the centrosomin-related protein mto1p. *Mol. Biol. Cell* **16**, 3040-3051.

Samejima, I., Miller, V. J., Groocock, L. M. and Sawin, K. E. (2008). Two distinct regions of Mto1 are required for normal microtubule nucleation and efficient association with the gamma-tubulin complex in vivo. *J. Cell Sci.* **121**, 3971-3980.

Samejima, I., Miller, V. J., Rincon, S. A. and Sawin, K. E. (2010). Fission yeast Mto1 regulates diversity of cytoplasmic microtubule organizing centers. *Curr. Biol.* **20**, 1959-1965.

Sawin, K. E., Lourenco, P. C. and Snaith, H. A. (2004). Microtubule nucleation at non-spindle pole body microtubule-organizing centers requires fission yeast centrosomin-related protein mod20p. *Curr. Biol.* **14**, 763-775.

Snaith, H. A. and Sawin, K. E. (2003). Fission yeast mod5p regulates polarized growth through anchoring of tea1p at cell tips. *Nature* **423**, 647-651.

Snaith, H. A., Anders, A., Samejima, I. and Sawin, K. E. (2010). New and old reagents for fluorescent protein tagging of microtubules in fission yeast; experimental and critical evaluation. *Methods Cell Biol.* **97**, 147-172.

Teixido-Travesa, N., Villen, J., Lacasa, C., Bertran, M. T., Archinti, M., Gygi, S. P., Caelles, C., Roig, J. and Luders, J. (2010). The {gamma}TuRC revisited: a comparative analysis of interphase and mitotic human {gamma}TuRC re-defines the set of core components and identifies the novel subunit GCP8. *Mol. Biol. Cell* **21**, 3963-3972.

Tischer, C., Brunner, D. and Dogterom, M. (2009). Force- and kinesin-8-dependent effects in the spatial regulation of fission yeast microtubule dynamics. *Mol. Syst. Biol.* **5**, 250.

Vardy, L. and Toda, T. (2000). The fission yeast gamma-tubulin complex is required in G(1) phase and is a component of the spindle assembly checkpoint. *EMBO J.* **19**, 6098-6111.

Venkatram, S., Tasto, J. J., Feoktistova, A., Jennings, J. L., Link, A. J. and Gould, K. L. (2004). Identification and characterization of two novel proteins affecting fission yeast gamma-tubulin complex function. *Mol. Biol. Cell* **15**, 2287-2301.

Wiese, C. and Zheng, Y. (2000). A new function for the gamma-tubulin ring complex as a microtubule minus-end cap. *Nat. Cell Biol.* **2**, 358-364.

Wiese, C. and Zheng, Y. (2006). Microtubule nucleation: gamma-tubulin and beyond. *J. Cell Sci.* **119**, 4143-4153.

Zheng, Y., Wong, M. L., Alberts, B. and Mitchison, T. (1995). Nucleation of microtubule assembly by a gamma-tubulin-containing ring complex. *Nature* **378**, 578-583.

Zimmerman, S. and Chang, F. (2005). Effects of {gamma}-tubulin complex proteins on microtubule nucleation and catastrophe in fission yeast. *Mol. Biol. Cell* **16**, 2719-2733.